Nonconventional Hydrogen Bonding

DOI: 10.1002/anie.201305710

Backbone FC–H···O Hydrogen Bonds in 2′F-Substituted Nucleic Acids**

Nerea Martin-Pintado, Glen F. Deleavey, Guillem Portella, Ramón Campos-Olivas, Modesto Orozco, Masad J. Damha, and Carlos González**

Stabilization of nucleic acid secondary structures results from a subtle balance of multiple interactions. Base pairing, base stacking, and cation binding have been extensively studied for decades, whereas the role of other interactions remains poorly understood.[1] Among them, nonconventional C–H···O hydrogen bonds are especially interesting. The importance of these interactions in proteins was recognized more than 40 years ago,[2] and during the last few years, several studies have shown their relevance in multiple biological structures.[3] In nucleic acids, most studies have focused on aromatic C–H···O interactions, and in particular, on the effect of non-conventional hydrogen bonds in base pairing and in base–sugar interactions.[3c,d,4] Backbone C–H···O hydrogen bonds have received less attention, although they have been proposed to play a role in the stabilization of four stranded i-motif structures,[5] and in tight packing of RNA and DNA elements.[6] Although these interactions are considered weak in natural nucleic acids, their strength can be increased through chemical modifications. Fluorine substitutions are particularly relevant, since fluorine provokes significant charge polarization effects in geminal and vicinal protons, an effect that has been well-characterized in small molecular systems.[7] Recently, Kakshoor et al. have observed fluorine-enhanced aromatic C–H···N interactions that significantly affect the strength of 2,4-difluorotoluene–adenine base pairs.[8] The prevalence of 2′-fluorinated oligonucleotides in nucleic acids research motivated us to examine the role of enhanced nonconventional hydrogen bonding in duplex stability.

Effects contributing to the enhanced thermal stability of 2′-deoxy-2′-fluororibonucleic acid (2′F-RNA) duplexes have been the subject of recent studies.[9] Recently, work by Egli and co-workers has demonstrated that 2′F-RNA duplex stabilization is primarily enthalpic in origin, through enhanced base stacking and pairing arising from long-range fluorine inductive effects on the nucleobases.[9,10] Stabilizing effects arising from fluorine have also been observed in the 2′ epimer of 2′F-RNA, 2′-deoxy-2′-fluoroarabinoonucleic acids (2′F-ANA). The geometry of 2′F-ANA:RNA duplexes are such that close 2′F···purine (H8) contacts are provoked, providing a very favorable geometry for hydrogen bond formation.[11]

Herein, we identify an additional stabilizing factor in A-form duplexes modified with 2′F-ANA and 2′F-RNA. Results demonstrate that fluorine-enhanced FC–H···O backbone interactions can have a strong stabilizing effect on oligonucleotide duplexes. Although close FC–H2′···O interactions have gone largely unnoticed, we propose that these interactions exist in other recently reported fluorinated duplexes,[9,11] and complement the enhanced base stacking and pairing effects stabilizing 2′F-RNA duplexes.

Two chimeric self-complementary duplexes containing continuous tracts (duplex **H**) and alternating regions (duplex **S**) of 2′F-ANA and 2′F-RNA residues (Figure 1 A and B) were used to carry out these structural, thermodynamic, and computational studies.

Self-complementary duplex formation and melting was monitored by UV absorbance at 260 nm and ^{1}H and ^{19}F NMR (Supporting Information, Figure S1 and S2). Melting temperature (T_m) values are shown in Table 1, showing that the T_m of **H** is over 20 °C greater than that of **S**, a trend in agreement

Table 1: T_m values and thermodynamic parameters for the self-complementary duplexes.[a]

Name	Sequence (5′-3′)[b]	T_m [°C]
D	5′-d(CGCGAATTCGCG)-3′	58.4
R	5′-r(CGCGAAUUCGCG)-3′	65.1
aF	5′-af(CGCGAATTCGCG)-3′	76.1
rF	5′-rf(CGCGAAUUCGCG)-3′	> 85
H	5′-rf(CGCGAA)-af(TTCGCG)-3′	70.4
S	5′-rf(CGCGAA)-afT-rfU-afC-rfG-afC-rfG-3′	48.8

[a] 4 μM oligonucleotide concentration, buffer conditions: 140 mM KCl, 1 mM $MgCl_2$ and 5 mM Na_2HPO_4, pH 7.2. [b] afN and rfN represent 2′F-ANA and 2′F-RNA units, respectively.

[*] Dr. N. Martin-Pintado, Prof. C. González
Instituto de Química Física "Rocasolano", CSIC
Serrano 119, 28006 Madrid (Spain)
E-mail: cgonzalez@iqfr.csic.es
Dr. G. F. Deleavey, Prof. M. J. Damha
Department of Chemistry, McGill University
801 Sherbrooke St. West, Montreal, QC H3A 0B8 (Canada)
E-mail: masad.damha@mcgill.ca
Dr. G. Portella, Prof. M. Orozco
Joint IRB-BSC program on Computational Biology, Institute for Research in Biomedicine, Barcelona Supercomputing Center, and Department of Biochemistry, University of Barcelona
Baldir i Reixac 10–12, 08028 Barcelona (Spain)
Dr. R. Campos-Olivas
Spectroscopy and NMR Unit, Spanish National Cancer Center (CNIO)
C/Melchor Fernández Almagro 3, 28029 Madrid (Spain)

[**] We thank the MICINN (CTQ2010-21567-C02-02 to C.G. and BIO2012-32868 to MO). CSIC I-LINK-0216 to C.G. and M.J.D., NSERC Discovery grant to M.J.D., a Vanier Canada Graduate Scholarship to G.F.D., a Sara Borrell fellowship to G.P., and a JAE-CSIC contract to N.M.P.

Supporting information for this article is available on the WWW under http://dx.doi.org/10.1002/anie.201305710.

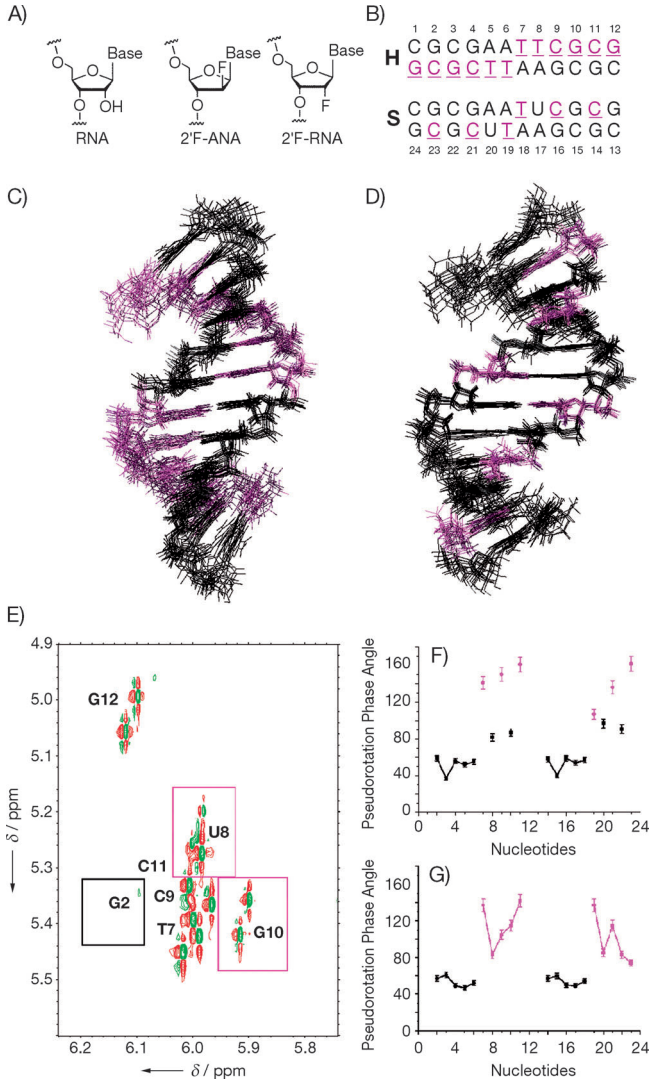

Figure 1. A) Structures of 2′F-ANA and 2′F-RNA in comparison with RNA. B) Numbering scheme of the 12-mer chimeric duplexes (**H** and **S**) used for this study. 2′F-ANAs are underlined in magenta and 2′F-RNAs are black. C), D) Ensemble of the 10 refined structures of **H** and **S**, respectively. E) Region of the DQF-COSY spectrum of **S** in D_2O showing H2′/H2″–H1′ cross-peaks (100 mM NaCl, 25 mM Na_2HPO_4, $T = 25\,°C$, pH 7). F), G) Pseudorotation phase angle versus sequence for the solution structures of **S** (F) and **H** (G).

with previous studies.[12] NMR spectroscopy, melting experiments, and non-denaturing gel electrophoresis clearly indicate that **H** and **S** form self-complementary duplexes in all of the conditions tested (Supporting Information, Figure S3 and S4), with formation of Watson–Crick base pairs, as shown by the cross-peak pattern in the NOESY spectra (Supporting Information, Figure S5 and S6).

Structural determination of **H** and **S** duplexes was accomplished to investigate their large difference in thermal stability (see the Supporting Information). The ten resulting structures are displayed in Figure 1 (PDB codes: 2M84, 2M8A). Structure calculation details are given in the Supporting Information, Table S3.

The structures of **H** and **S** are intermediate between canonical A and B forms and retain structural features of both families of double helical structures (Figure 1; Supporting Information, Figure S8). The geometry of 2′F-RNA nucleotides in the continuous tracts of **H** and **S** is very similar to that expected for an RNA homoduplex, with riboses adopting the expected C3′-*endo* conformation (phase angles about 40–60°; Figure 1; Supporting Information, Figure S9). Interestingly, 2′F-ribose conformations of alternating 2′F-ANA/2′F-RNA steps in **S** fall within the east domain, with pseudorotation phase angles between 80° and 95°. This unexpected ribose conformational switch arising in the steps region is fully consistent with the experimental *J*-coupling data (Figure 1). The 2′F-arabinoses adopt south/east conformation, with pseudorotation phase angles between 75° and 140° in **H**, and 100° to 160° in **S**. Geometrical parameters are shown in the Supporting Information, Tables S4–S9.

As 2′F-ANA and 2′F-RNA nucleotides are considered, respectively, as DNA and RNA analogues, it is interesting to compare the structures of the 2′F-ANA:2′F-RNA segments of **H** with that of 2′F-ANA:RNA hybrids. In the structure of a 2′F-ANA:RNA hybrid decamer (PDB ID: 2KP4),[11] 2′F-ANA nucleotides adopt an east sugar conformation and glycosidic angles between 110° and 120°, provoking a close 2′F···H8 contact, with a 2′F···H8–C angle of about 150° that favors hydrogen bond formation.[11] In contrast, glycosidic angles of contiguous tracts of 2′F-ANA residues in **H** are between 130° and 140° (Supporting Information, Figure S9). These higher *anti* values in **H** are typical of a pure A duplex and prevent the appropriate orientation for 2′F···H8–C hydrogen bond formation. The experimental evidence for this interaction in 2′F-ANA:RNA hybrids arises from strong sequential 2′F-H8 HOE cross-peaks and heteronuclear ^{19}F–^{1}H *J*-couplings for inter and intra interactions, respectively. None of these are observed in the 2′F-ANA:2′F-RNA chimeric duplex **H** (Supporting Information, Figure S7).

On the other hand, very close contacts between H2′ in 2′F-RNA and H2″ in 2′F-ANA and their 3′-neighbor O4′-sugar and O5′-backbone atoms are observed in the continuous tracts of 2′F-ANA or 2′F-RNA (Figure 2). The H2″···O distances are particularly short in 2′F-ANA tracts (about 2.8 Å excluding the terminal residue), where the C–H2″···O4′ angles are close to co-linearity (average of 160°; see Table 2 and Supporting Information, Tables S10 and S11 for details). Owing to the high fluorine electronegativity, the geminal H2′/H2″ in 2′F-ANA and 2′F-RNA nucleotides are positively polarized, provoking a favorable electrostatic interaction with the surrounding electron dense oxygen atoms in the oligonucleotide backbone (Figure 2). In particular, the C–H···O4′ geometry (Table 2) resembles that of nonconventional C–H···O hydrogen bonds observed in different contexts.[3a] In our case, the positive charge polarization of H2′/H2″ protons induced by the geminal 2′F is supported by their NMR chemical shifts, which in 2′F-ANA and 2′F-RNA exhibit significant downfield shifts (5–6 ppm) compared to those typically observed in RNA (4 ppm).

The dramatic impact of these sequential C–H···O interactions on duplex stability becomes apparent when the structures of the **H** and **S** duplexes are compared. The

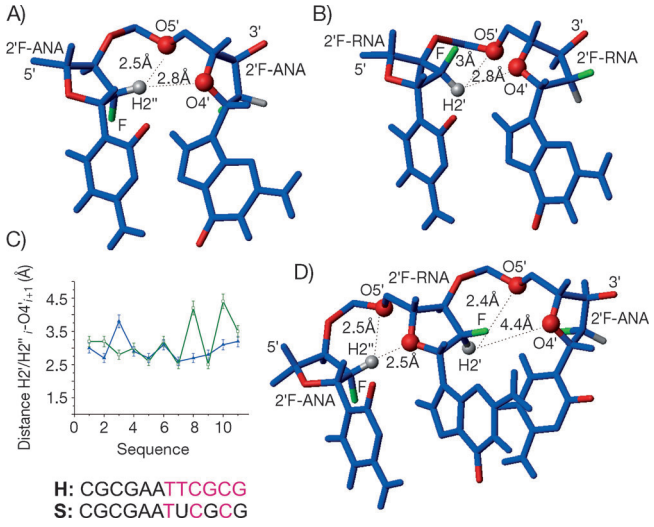

Figure 2. View of short distances between H2′/H2″$_i$···O4′/O5′$_{i+1}$ oxygen atoms in A) 2′F-ANA and B) 2′F-RNA continuous tracts of **H** and **S**, respectively. C) Values of H2′/H2″$_i$···O4′$_{i+1}$ distances all along the sequence (2′F-RNA in black and 2′F-ANA in magenta) in **H** (blue) and **S** (green). D) Structure and view of distances in steps of **S**. C blue, H gray, O red, F green.

Table 2: Average values of H2′/H2″$_i$···O4′$_{i+1}$ distances [Å], angles between C–H2′/H2″$_i$···O4′$_{i+1}$ in different structures, and topological properties of the bond critical points (BCP) detected between the H2′/H2″$_i$···O4′$_{i+1}$.[a]

Step	Structure	Distance H2′/H2″···O4′	Angle C2′H2′/H2″···O4′	ρ [au]	$\nabla^2\rho$ [au]
RNA$_i$/RNA$_{i+1}$	Pure RNA (PDB: 1RXB)	2.5	144	0.005435	0.020660
2′F-RNA$_i$/2′F-RNA$_{i+1}$	Pure 2′F-RNA (PDB:3P4A)	2.6	140	0.010307	0.034542
2′F-RNA$_i$/2′F-RNA$_{i+1}$	H, S	2.9	110	0.007085	0.027376
2′F-ANA$_i$/2′F-ANA$_{i+1}$	H	2.8	160	0.004617	0.017697
2′F-ANA$_i$/2′F-RNA$_{i+1}$	S	2.5	147	0.007612	0.027338
2′F-RNA$_i$/2′F-ANA$_{i+1}$	S	4.4	73	n.d.	n.d.
2′F-ANA$_i$/2′F-ANA$_{i+1}$	2′F-ANA:RNA hybrid	2.9	146	n.c.	n.c.
2′F-RNA$_i$/2′F-RNA$_{i+1}$	Standard A-type	2.9	120	n.c.	n.c.
2′F-ANA$_i$/2′F-ANA$_{i+1}$	Standard B-type	4.7	107	n.c.	n.c.

[a] n.d.: not detected; n.c.: not calculated.

favorable H2′$_i$···O4′$_{i+1}$ contacts (2.9 Å) observed in the continuous tracts are disrupted in some of the 2′F-RNA$_i$/2′F-ANA$_{i+1}$ junctions (8→9 and 10→11) of duplex **S** (H2′$_i$···O4′$_{i+1}$ distance around 4.4 Å) (Figure 2 and Table 2). These distances are closely connected with the sugar conformations in 2′F-ANA/2′F-RNA and in 2′F-RNA/2′F-ANA junctions. Alternation of south 2′-fluoroarabinoses and east 2′-fluororiboses favors C-H2″···O4′ contacts in 2′F-ANA$_i$/2′F-RNA$_{i+1}$ steps, and prevents their formation in the adjacent 2′F-RNA$_i$/2′F-ANA$_{i+1}$ step (Figure 2 D). Furthermore, since fluorine inductive effects might be dependent on the 1,2-diaxial disposition of the fluorine,[13] the induction felt by the nucleobases of east conformers of 2′F-RNA (and south conformers of 2′F-ANA) could be reduced. Thus, the east 2′F-RNA residues observed in the **S** duplex may lack both enhanced stacking and an FC–H···O interaction with the 3′ neighboring 2′F-ANA nucleotide, both of which contribute to the large difference in stability between **H** and **S** (ΔT_m = 21.6 °C).

Interestingly, as seen in the **S** duplex, flanking 2′F-ANA modifications can invoke an unprecedented east conformation in 2′F-RNA. The pseudorotation energy profile resulting from QM calculation indicates that such conformation is unfavorable (Supporting Information, Figure S10 and S11). However, east puckered 2′F-RNA residues allows the formation of optimal FC–H2″···O4′ contacts in 2′F-ANA$_i$/2′F-RNA$_{i+1}$ steps (Table 2).

Close FC–H2′···O contacts most likely contribute to the enhanced stability reported in the crystallographic structures of a pure 2′F-RNA duplex and a chimeric 2′F-RNA/RNA duplex.[9] H2′$_i$···O4′$_{i+1}$ distances are about 2.6 Å (Table 2; Supporting Information, Tables S12 and S13), and the C–H2′$_i$···O4′$_{i+1}$ angles are about 140° (Supporting Information, Figure S12); both are consistent with hydrogen bond formation. The two structures are pure A form with all of the sugars in the north conformation. Similarly, close H2″$_i$···O4′$_{i+1}$ distances and a co-linear arrangement of C-H2″$_i$···O4′$_{i+1}$ is observed in the solution structure of a 2′F-ANA:RNA hybrid (Table 2; Supporting Information, Table S15). In this case, the overall structure of the duplex is intermediate between A and B forms, and 2′F-arabinoses adopt the east conformation.[11] These contacts are not observed in the structure of 2′F-ANA:2′F-ANA duplexes, where the global structure is the B-form and the arabinoses adopt the south conformation (Table 2).[14] Taking together all of these observations, we conclude that sequential FC–H···O4′ interactions are favored in the A-form (such as 2′F-RNA:2′F-RNA) or A-like hybrids (such as 2′F-ANA:RNA).

To address whether these FC–H···O interactions are real hydrogen bonds, we carried out quantum-mechanical calculations in dinucleotide model systems that mimic the four possible step combinations that occur in **H** and **S**, that is, 2′F-RNA$_i$/2′F-RNA$_{i+1}$, 2′F-ANA$_i$/2′F-ANA$_{i+1}$, 2′F-RNA$_i$/2′F-ANA$_{i+1}$, and 2′F-ANA$_i$/2′F-RNA$_{i+1}$. We have also included 2′F-RNA$_i$/2′F-RNA$_{i+1}$, and RNA$_i$/RNA$_{i+1}$ dinucleotides from the high-resolution X-ray structures of a pure 2′F-RNA duplex and a RNA duplex, respectively (Supporting Information, Figure S12–13 and Tables S12 and S14).[9,15]

To detect potential stabilizing interactions in these systems, we analyzed the electron density of the optimized dinucleotide steps by means of the theory of "atoms in molecules".[16] Values of the electron density (ρ) and the Laplacian of the electron density ($\nabla^2\rho$) for the observed BCPs in each dinucleotide step are listed in Table 2. The presence of BCPs is a necessary condition to identify stabilizing noncovalent interactions. In the case of hydrogen bonds, the electron density in the BCP of a hydrogen bond ranges from 0.002 to 0.011 atomic units (au), and the

Laplacian of the charge density is known to be positive and in the range of 0.014 to 0.139 au.[17] Values shown in Table 2 are within this range, indicating the presence of a sequential FC–H···O hydrogen bond, in all step types except 2′F-RNA$_i$/2′F-ANA$_{i+1}$. These values are in agreement with those reported for small-molecular-weight systems,[7a] and indicate that FC–H···O hydrogen bonds in 2′F-RNA$_i$/2′F-RNA$_{i+1}$ and 2′F-ANA$_i$/2′F-RNA$_{i+1}$ steps are between 1 to 2 kcal mol^{-1} more stabilizing than C–H$_i$···O$_{i+1}$ hydrogen bonds in RNA$_i$/RNA$_{i+1}$ steps.

In conclusion, the results presented herein reveal that FC–H···O hydrogen bonds have a strong stabilizing effect on 2′-fluorinated duplexes. The detailed structural analysis of two oligonucleotides containing alternate and contiguous tracts of 2′F-RNA and 2′F-ANA shows that the disruption of FC–H···O hydrogen bonds in 2′F-RNA/2′F-ANA steps destabilize the duplex, providing a means to tune siRNA thermal stability and gene silencing activity.[12] It is worth mentioning that these FC–H···O interactions are not restricted to duplex structures, but they can also provoke a strong stabilization of parallel G-quadruplexes.[18] This FC–H···O effect might be involved in the stabilization of other noncanonical structures, such as i-motifs where sugar–sugar contacts are of particular relevance.[5] Clearly, the existence of noncanonical H-bonds in these fluorinated structures appears to make a beneficial contribution to stability, providing additional insight on the structural nature of fluorinated oligonucleotides.

Received: July 2, 2013
Revised: July 29, 2013
Published online: September 23, 2013

Keywords: DNA structures · hydrogen bonding · modified nucleic acids · NMR spectroscopy

[1] a) E. T. Kool, *Annu. Rev. Biophys. Biomol. Struct.* **2001**, *30*, 1–22; b) J. Šponer, J. Leszczynski, P. Hobza, *Biopolymers* **2001**, *61*, 3–31; c) E. T. Kool, *Chem. Rev.* **1997**, *97*, 1473–1488.

[2] a) G. N. Ramachandran, V. Sasisekharan, *Biochim. Biophys. Acta Biophys. Photosyn.* **1965**, *109*, 314–316; b) S. Krimm, *Science* **1967**, *158*, 530–531.

[3] a) S. Horowitz, R. C. Trievel, *J. Biol. Chem.* **2012**, *287*, 41576–41582; b) M. C. Wahl, M. Sundaralingam, *Trends Biochem. Sci.* **1997**, *22*, 97–102; c) J. M. Benevides, G. J. Thomas, *Biochemistry* **1988**, *27*, 3868–3873; d) A. Ghosh, M. Bansal, *J. Mol. Biol.* **1999**, *294*, 1149–1158.

[4] a) J. R. Quinn, S. C. Zimmerman, J. E. Del Bene, I. Shavitt, *J. Am. Chem. Soc.* **2007**, *129*, 934–941; b) Y. P. Yurenko, R. O. Zhurakivsky, S. P. Samijlenko, D. M. Hovorun, *J. Biomol. Struct. Dyn.* **2011**, *29*, 51–65.

[5] I. Berger, M. Egli, A. Rich, *Proc. Natl. Acad. Sci. USA* **1996**, *93*, 12116–12121.

[6] I. Berger, M. Egli, *Chem. Eur. J.* **1997**, *3*, 1400–1404.

[7] a) Y. Gu, T. Kar, S. Scheiner, *J. Am. Chem. Soc.* **1999**, *121*, 9411–9422; b) E. Cubero, M. Orozco, F. J. Luque, *Chem. Phys. Lett.* **1999**, *310*, 445–450; c) C. Dalvit, A. Vulpetti, *ChemMedChem* **2011**, *6*, 104–114.

[8] O. Khakshoor, S. E. Wheeler, K. N. Houk, E. T. Kool, *J. Am. Chem. Soc.* **2012**, *134*, 3154–3163.

[9] P. S. Pallan, E. M. Greene, P. A. Jicman, R. K. Pandey, M. Manoharan, E. Rozners, M. Egli, *Nucleic Acids Res.* **2011**, *39*, 3482–3495.

[10] A. Patra, M. Paolillo, K. Charisse, M. Manoharan, E. Rozners, M. Egli, *Angew. Chem.* **2012**, *124*, 12033–12036; *Angew. Chem. Int. Ed.* **2012**, *51*, 11863–11866.

[11] J. K. Watts, N. Martín-Pintado, I. Gómez-Pinto, J. Schwartzentruber, G. Portella, M. Orozco, C. González, M. J. Damha, *Nucleic Acids Res.* **2010**, *38*, 2498–2511.

[12] a) G. F. Deleavey, J. K. Watts, T. Alain, F. Robert, A. Kalota, V. Aishwarya, J. Pelletier, A. M. Gewirtz, N. Sonenberg, M. J. Damha, *Nucleic Acids Res.* **2010**, *38*, 4547–4557; b) H. Ikeda, R. Fernandez, J. J. Barchi, X. Huang, V. E. Marquez, A. Wilk, *Nucleic Acids Res.* **1998**, *26*, 2237–2244.

[13] J. Graton, Z. Wang, A. M. Brossard, D. Goncalves Monteiro, J. Y. Le Questel, B. Linclau, *Angew. Chem.* **2012**, *124*, 6280–6284; *Angew. Chem. Int. Ed.* **2012**, *51*, 6176–6180.

[14] N. Martín-Pintado, M. Yahyaee-Anzahaee, R. Campos-Olivas, A. M. Noronha, C. J. Wilds, M. J. Damha, C. González, *Nucleic Acids Res.* **2012**, *40*, 9329–9339.

[15] S. Portmann, N. Usman, M. Egli, *Biochemistry* **1995**, *34*, 7569–7575.

[16] R. F. W. Bader, *Atoms in Molecules—A Quantum Theory*, Clarendon, Oxford, UK, **1990**.

[17] E. Cubero, M. Orozco, P. Hobza, F. J. Luque, *J. Phys. Chem. A* **1999**, *103*, 6394–6401.

[18] N. Martín-Pintado, M. Yahyaee-Anzahaee, G. F. Deleavey, G. Portella, M. Orozco, M. J. Damha, C. González, *J. Am. Chem. Soc.* **2013**, *135*, 5344–5347.

